Journal of Chromatography A, 1568 (2018) 91–100

Contents lists available at ScienceDirect

Journal of Chromatography A

journal homepage: www.elsevier.com/locate/chroma

Lipidomic alterations in lipoproteins of patients with mild cognitive impairment and Alzheimer's disease by asymmetrical flow field-flow fractionation and nanoflow ultrahigh performance liquid chromatography-tandem mass spectrometry

San Ha Kim [a], Joon Seon Yang [a], Jong Cheol Lee [a], Ji-Yeon Lee [b], Jun-Young Lee [b,c,**], Eosu Kim [d], Myeong Hee Moon [a,*]

[a] Department of Chemistry, Yonsei University, Seoul 03722, Republic of Korea
[b] Department of Psychiatry, SMG-SNU Boramae Medical Center, Seoul 07061, Republic of Korea
[c] Department of Psychiatry and Neuroscience Research Institute, Seoul National University College of Medicine, Seoul 03080, Republic of Korea
[d] Department of Psychiatry, Institute of Behavioral Science in Medicine, Yonsei University College of Medicine, Seoul 03722, Republic of Korea

ARTICLE INFO

Article history:
Received 20 March 2018
Received in revised form 22 June 2018
Accepted 4 July 2018
Available online 5 July 2018

Keywords:
Lipidomics
Lipoproteins
Alzheimer's disease
Mild cognitive impairment
Flow field-flow fractionation
nUHPLC-ESI-MS/MS

ABSTRACT

Alzheimer's disease (AD) is an irreversible neurodegenerative disorder with the clinical symptom of the progressive loss of cognitive function and mild cognitive impairment (MCI) is a translational state between cognitive changes of normal aging and AD. Lipid metabolism and pathogenesis of Alzheimer's disease (AD) are closely linked. Despite obviously discrete lipidome constitutions across lipoproteins, lipidomic approaches of AD has been mostly conducted without considering lipoprotein-dependent alterations. This study introduces a combination of asymmetrical flow field-flow fractionation (AF4) and nanoflow ultrahigh performance liquid chromatography-tandem mass spectrometry (nUHPLC-ESI-MS/MS) for a comprehensive lipid profiling in different lipoprotein level of patients plasma with AD and amnestic MCI in comparison to age-matched healthy controls. Lipoproteins in plasma samples were size-sorted by a semi-preparative scale AF4, followed by non-targeted lipid identification and high speed targeted quantitation with nUHPLC-ESI-MS/MS. It shows 14 significantly altered high abundance lipids in AD, exhibiting >2-fold increases ($p < 0.01$) in LDL/VLDL including triacylglycerol, ceramide, phosphatidylethanolamine, and diacylglycerol. Three lipid species (triacylglycerol 50:1, diacylglycerol 18:1_18:1, and phosphatidylethanolamine 36:2) showing a strong correlation with the degree of brain atrophy were found as candidate species which can be utilized to differentiate the early stage of MCI when simple Mini-Mental State Examination results were statistically incorporated. The present study elucidated lipoprotein-dependent alterations of lipids in progression of MCI and further to AD which can be utilized for the future development of lipid biomarkers to enhance the predictability of disease progress.

1. Introduction

Alzheimer's disease (AD) is an irreversible neurodegenerative disorder that is the most common cause of dementia in adults older than 65 years of age; notably, it presents a challenging task for health care in the developed countries, since it will dramatically increase in the future [1–3]. The clinical symptoms of AD comprise a progressive loss of cognitive function, typically memory; AD is pathologically distinguished by an extensive loss of synapses and neurons, as well as by the presence of neuritic plaques enriched with amyloid β (Aβ) peptides in brain [4] and of neurofibrillary tangles composed of hyperphosphorylated tau proteins [5]. Mild cognitive impairment (MCI) refers to a transitional state between the cognitive changes of normal aging and AD. Because 80% of MCI has been reported to progress to AD over a period of 6 years [6], and changes in the brain caused by AD pathogenesis may occur earlier than the onset of MCI symptoms [7], the identification of the earliest signs of disease progression is important in establishing preven-

* Corresponding authorat : Department of Chemistry, Yonsei University, Seoul 03722, Republic of Korea.
** Co-corresponding author at: Department of Psychiatry and Neuroscience Research Institute, Seoul National University College of Medicine, Seoul 03080, Republic of Korea.
E-mail addresses: benji@snu.ac.kr (J.-Y. Lee), mhmoon@yonsei.ac.kr (M.H. Moon).

https://doi.org/10.1016/j.chroma.2018.07.018
0021-9673/

tive treatments for potential AD patients [8,9]. Therefore, reliable and convenient blood biomarkers, which clinicians could use to predict the potential of AD development, are crucial to enable the commencement of preventive intervention at the earliest stages.

Although several AD biomarkers, such as Aβ peptides and tau protein have been developed using cerebrospinal fluid (CSF) [10–13], lumbar puncture to obtain CSF is rather invasive. Few plasma proteins, based on proteomic approaches have been reported to predict the progression of MCI to AD [9,14,15]; however, most of them require further clinical validation. Alterations in lipid levels are known to modulate the generation of Aβ [3,16,17]. Studies show decreased levels of phosphatidylethanolamine plasmalogen and sulfatide, but increases in ceramide and diacylglycerol, in the AD-brain or CSF [3,18–20], as well as few putative lipid signatures from AD-plasma [21]. Also reported are higher levels of low-density lipoprotein (LDL) cholesterol, which is closely linked with AD [22]. While the roles and consequences of lipids in AD have been described, detailed profiles of blood lipids with AD, especially those of different lipoproteins, have not yet been thoroughly investigated.

Lipid analysis at the molecular level is often complicated, due to the diversity in lipid molecular structures. Rapid growth in mass spectrometry (MS) has facilitated lipidomic analysis. Direct analysis of lipids using electrospray ionization-tandem MS (ESI-MS/MS) provides the high throughput analysis and the accurate determination of lipid molecular structures [23,24], however, it can not avoid the ion suppression effect caused by high abundance lipid species and the difficulty in identifying isobaric lipids. Lipid analysis has been empowered by hyphenating chromatographic methods with ESI-MS/MS such as reversed phase liquid chromatography (RPLC) in most cases, hydrophilic-interaction liquid chromatography (HILIC), supercritical fluid chromatography (SFC), two-dimensional LC, and etc. [25–31]. Lately, we have demonstrated that nanoflow ultrahigh performance liquid chromatography-electrospray ionization-tandem mass spectrometry (nUHPLC-ESI-MS/MS) can facilitate the identification of lipid structures at low fmol levels with a high speed quantitation: lipid profiles in the plasma of patients with Gaucher diseases upon enzyme replacement therapy, in the muscle tissues of diabetic rats upon physical exercise, and in urinary exosomes from patients with prostate cancer [32–34].

In this study, a comprehensive targeted profiling of lipids has been performed with human plasma lipoproteins of patients who were diagnosed with AD and MCI in comparison to age-matched healthy controls. Lipoproteins were size-sorted into high density lipoprotein (HDL) and LDL including very low-density lipoprotein (VLDL) using semi-preparative scale asymmetrical flow field-flow fractionation (AF4), an elution-based size-separation technique [35]. Then, lipids in HDL and LDL/VLDL were analyzed for non-targeted identification of molecular structures, followed by targeted quantitation using nUHPLC-ESI-MS/MS based on selective reaction monitoring method and statistical evaluation of the dependence of lipids with brain damage. This study aimed to elucidate the lipoprotein-dependent lipids in the progression of MCI and AD, which can be utilized in the future as candidate molecules to enhance the predictability of disease by engaging with the mini-mental state examination (MMSE) results.

2. Experimental

2.1. Materials & reagents

A total of 25 lipid standards were used to optimize nUHPLC-ESI-MS/MS run conditions, together with 14 internal standards having odd-numbered acyl chains. These were lysophosphatidylcholine (LPC) 12:0, phosphatidylcholine (PC) 13:0/13:0, PC 16:0/14:0, PC 16:0/16:0, PC 18:1/18:0, PC 20:0/20:0, lysophophatidylethanolamine (LPE) 14:0, phophatidylethanolamine (PE) 12:0/12:0, phophatidylethanolamine plasmalogen (PEp) 18:0p/18:1, lysophosphatidic acid (LPA) 14:0, phosphatidic acid (PA) 12:0/12:0, lysophosphatidylglycerol (LPG) 14:0, phosphatidylglycerol (PG) 15:0/15:0, PG 16:0/16:0, lysophosphatidylinositol (LPI) 18:0, phosphatidylinositol (PI) 16:0/18:2, lysophosphatidylserine (LPS) 18:1, phosphatidylserine (LPS) 18:0/18:1, sulfatide (SulfoHexCer) d18:1/12:0, ceramide (Cer) d18:1/14:0, monohexosylceramide (HexCer) d18:1/16:0, dihexosylceramide (Hex2Cer) d18:1/16:0, cardiolipin (CL) $(14:0)_4$, diacylglycerol (DG) 16:0/18:1, and triacylglycerol (TG) 16:0/16:0/14:1. Lipids used for internal standards at selected reaction monitoring (SRM) were LPC 17:0, LPE 17:1, PE 17:0/17:0, LPA 17:0, PA 17:0/17:0, LPG 17:1, PI 17:0/20:4, SulfoHexCer d18:1/17:0, SM d18:1/17:0, Cer d18:1/17:0, HexCer d18:1/17:0, CL $(14:1)_3(15:1)$, DG 17:0/17:0-D_5, and TG 17:0/17:1/17:0-D_5. All lipid standards were purchased from Avanti Polar Lipids, Inc. (Alabaster, AL, USA). Standard materials of bovine serum albumin (BSA), lipoprotein standard high-density lipoprotein (HDL), and low-density lipoprotein (LDL) were purchased from Sigma-Aldrich Co. (St. Louis, MO), and very low-density lipoprotein (VLDL) was from Merck Millipore (Darmstadt, Germany). Methyl-*tert*-butyl ether (MTBE), $CHCl_3$, NH_4HCO_2, and NH_4OH were purchased from Sigma-Aldrich. HPLC grade H_2O, CH_3CN, $(CH_3)_2CHOH$, and CH_3OH were purchased from J.T. Baker, Inc. (Phillipsburg, NJ, USA). Capillary tubes (inner diameter: 25 and 100 μm, outer diameter: 360 μm) were purchased from Polymicro Technologies, LLC (Phoenix, AZ).

2.2. Patient's plasma sample

From a total of 172 participants recruited in a memory clinic of University-affiliated general hospital (Seoul, Korea) with informed consent according to the permission of the Institutional Review Boards, 13 individuals (age = 71.5 ± 3.6) with normal cognition, 23 (age = 72.5 ± 3.1) with MCI, and 14 (age = 72.6 ± 3.1) with AD were finally selected. Inclusion criteria were female (65–80 years) with Clinical Dementia Rating (CDR) of 0–1.0. Exclusion criteria were 1) history of major psychiatric or neurologic illness (stroke, head trauma, epilepsy), 2) significant medical condition that may affect mental functioning, 3) no current diagnosis of diabetes, and 4) CDR ≥ 2.0. In addition, patients with hyperlipidemia or a high level of BMI were not included in order to reduce the influences of obesity or hyperlipidemia on the lipid profiles. The study was conducted in accordance with the current version of the Declaration of Helsinki. Demographic data for selected plasma samples are listed in Table S1 of Supplementary material.

Overnight fasting blood samples were collected in the morning (around 10 a.m.) by venipuncture at antecubital vein. Plasma was immediately prepared by centrifuge (2000 × *g*) for 15 min from whole blood collected in a heparin tube after gently mixing. Plasma was allocated into several Eppendorf tubes by 0.7 cc each and immediately stored in −80 °C. Blood sample for genotyping was collected into an EDTA tube, allocated into Eppendorf tubes and stored in −80 °C. APOE ε4 genotyping was performed from whole blood as described previously [36]. Rest of blood sample was immediately sent to clinical laboratory for routine blood tests including complete blood cell count, BUN/creatinine, albumin, liver function tests, fasting serum glucose, glycated hemoglobin (HbA1c), serum lipids, homocysteine, thyroid function test etc.

2.3. Neuropsychological & neuroimaging assessment

All participants were evaluated and diagnosed by trained board-certified psychiatrists, based on clinical interview and results from neuropsychological tests, neuroimaging (magnetic resonance imaging, MRI) studies, and blood tests, together with CDR global score and CDR-Sum-of-boxes [37], Mini-Mental State Examination [38,39], and the Consortium to Establish a Registry for Alzheimer's disease (CERAD) [40] neuropsychological batteries. Diagnostic classification (control, MCI, and AD) was conducted based on the National Institute of Neurological and Communicative Disorders and Stroke and the Alzheimer's Disease and Related Disorders Association (NINCDS-ADRDA) criteria [41] and on Peterson's criteria for MCI [42].

Structural brain MRI, including T1-weighted, T2-weighted, and fluid-attenuated inversion recovery (FLAIR) sequences, were obtained on a 3.0 T scanner (Intera Achieva; Philips Medical Systems, Best, The Netherlands). The degree of atrophy of the medial temporal lobe (MTA) was rated by the visual rating: 0 (none), 1 (equivocal), 2 (mild), 3 (severe), and 4 (severe) in right and left brain by Scheltens criteria [43]. White matter hyperintensity was rated separately regarding deep white matter hyperintensity (DWH) and periventricular hyperintensity (PVH) according to a previous method [44]: 0 (none), 1 (mild), 2 (moderate), and 3 (severe).

2.4. Size fractionation of lipoproteins by AF4

Size-separation and collection of HDL and LDL/VLDL fractions was achieved with semi-preparative scale AF4 channel system with the depleted plasma sample. Prior to size sorting of lipoproteins from plasma samples, albumin and immunoglobulin G (IgG) were depleted by using ProteoPrep® Immunoaffinity Albumin & IgG Depletion Kit from Sigma-Aldrich. Collection periods were established from AF4 separation of stained plasma samples, of which lipoproteins were preliminary stained with Sudan Black B (SBB) for the detection of lipoproteins at $\lambda = 600$ nm using a model 730D UV detector from Young-Lin Instrument (Seoul, Korea). The semi-preparative scale AF4 channel (model Eclipse® Channel SP3, 26.6 cm long) from Wyatt Technology Europe GmbH (Dernbach, Germany) was utilized with a regenerated cellulose membrane (MWCO 10 kDa) purchased from Millipore (Danvers, MA). The channel spacer was made from a 250 μm thick polyvinyl chloride (PVC) sheet cut to 4.4 cm in initial breadth with a trapezoidal decrease to a final breadth of 0.4 cm. An SP930D HPLC pump from Young-Lin Instrument (Seoul, Korea) delivered carrier liquid to the channel via a model 7125 loop injector from Rheodyne (Cotati, CA, USA). The carrier liquid was 0.1 M phosphate buffered saline (PBS) solution prepared with ultrapure water (>18 MΩ cm) and was filtered with 0.22 μm nitrocellulose membrane filter from EMD Millipore (Billerica, MA, USA) prior to use. 50 μL of raw plasma sample was injected to AF4 channel and the collection of HDL and LDL/VLDL fractions were made twice for each sample. Thus, a total of 100 μL of each plasma sample was utilized for the collection of lipoproteins.

2.5. Lipid extraction from lipoprotein

Each lipoprotein fraction was concentrated to a final volume of approximately 500 μL for each sample, using Amicon Centrifugal Filters (MWCO 10 kDa) from Millipore. The modified Folch method, using MTBE/CH_3OH [45], was used to extract lipids from the collected lipoprotein fractions. The concentrated lipoprotein solution was transferred to 2 mL tube. 300 μL of CH_3OH was added the solution and then it was vortexed briefly. The tube was placed in an ice bath for 10 min. 1000 μL of MTBE was added to the tube and the mixture was vortexed for 1 h at 25 °C. 250 μL of MS-grade H_2O was added to the tube, followed by vortexing for 10 min. and then centrifugation ($1000 \times g$) for 10 min. The upper organic layer was pipetted out and transferred to a pre-weighed tube. 300 μL of MTBE was added to the remaining aqueous layer and the mixture was tip-sonicated for 2 min. After centrifuge ($1000 \times g$) for 10 min, the upper organic layer was pipetted out and transferred to the previously collected organic layer. The tube was sealed with 0.45 μm MilliWrap PTFE membrane from Millipore to avoid lipid evaporation during lyophilization for 12 h. Lyophilized lipids were weighed, reconstituted in CH_3OH:$CHCl_3$ (9:1, v/v), and stored at −80 °C. For nUHPLC-ESI-MS/MS analysis, each frozen sample was diluted to 5 μg/μL with CH_3OH:H_2O (8:2, v/v).

2.6. Nanoflow UHPLC-ESI-MS/MS of lipids

Lipid analysis was performed in two steps. At first, global identification of lipid molecular structure was made for the lipid extract of HDL and LDL/VLDL fractions collected from the control, MCI, and AD groups by using nUHPLC-ESI-MS/MS: A Dionex Ultimate 3000 RSLCnano System with an autosampler coupled with LTQ Velos ion trap mass spectrometer from Thermo Scientific™ (San Jose, CA, USA). Homemade capillary columns were prepared with a fused silica capillary tube (100 μm I.D. and 360 μm O.D.) from Polymicro Technologies, LLC (Phoenix, AZ). Prior to packing, one end of capillary tube was pulled by flame to make a sharp needle for a direct ESI emitter. For column packing, Watchers® ODS-P C18 particles (3 μm) from Isu Industry Corp. (Seoul, Korea) was packed for the first 0.5 cm from the pulled tip to make self-assembled frit and then packed with 1.7 μm C18 particles (130 Å) which were unpacked from XBridge® BEH C18 from Waters for 7 cm under nitrogen gas at 1000 psi. The connection of the analytical column with a capillary tube from UHPLC was made with a micro-cross from IDEX Health & Science (Oak Harbor, WA, USA) by linking a Pt wire for ESI voltage at one port and a vent tube at the remaining port leading to the on/off switching valve to split flow. Mobile phase solutions for gradient elution were (9:1, v/v) H_2O:CH_3CN for A and (2:2:6, v/v/v) CH_3OH:CH_3CN:IPA for B, which were added with a mixed ionization modifier, 5 mM NH_4HCO_2 and 0.05% NH_4OH. Lipid extract sample was loaded to an analytical column directly by using mobile phase A at 650 nL/min with the on/off valve closed for 15 min and then the pump flow was raised to 6.5 μL/min with the on/off valve open so that only 300 nL/min of flow was allowed to the analytical column. Gradient elution began by ramping mobile phase B to 40% for 2 min, increasing it to 80% for 10 min/6 min (positive/negative ion mode), then to 99% for 20 min/10 min, and it was maintained at 99% for 10 min/15 min. Then it was resumed to mobile phase A and reconditioned for 7 min for both ion modes. Applied ESI voltage was 3.0 kV and 40% of normalized collision energy was for non-targeted identification of lipids. Mass range was 350–1100 amu for positive ion mode and 300–1100 amu for negative ion mode. Molecular structures of lipids were determined by LiPilot, a computer software program developed in our laboratory [46], followed by manually verification.

Targeted quantitation of identified lipids was made for individual samples using a model nanoACQUITY UPLC system from Waters™ (Milford, MA, USA), equipped with a TSQ Vantage triple-stage quadrupole MS system from Thermo Scientific™ utilizing the same analytical column utilized for the non-targeted analysis. For gradient elution, the pump flow rate employed was 15 μL/min but only 300 nL/min of flow was delivered to the column. Gradient elution began by ramping the mobile phase B to 50% for 1 min, to 80% for 10 min, further to 100% for 15 min, and it was maintained for 15 min. Selected reaction monitoring (SRM)-based quantification was performed by analyzing precursor and product ions in data-dependent collision induced dissociation (CID) experiments

in positive and negative ion modes alternatively in a single run using a scan width at *m/z* 1.5, scan time at 0.001 s, and ESI voltage of 3 kV. Lipid classes of LPG, PG, LPI, PI, LPA, PA, and CL were analyzed at negative ion mode and those of The LPC, PC, LPE, PE, PEp, DG, TG, Cer, SM, HexCer, Hex2Cer, and SulfoHexCer were at positive ion mode. Collision energy was differently applied depending on the type of lipid classes: 20 V for LPE, PE, and PEp; 25 V for LPA, and LPC; 30 V for LPG; 35 V for PG, DG, and TG; 40 V for PA, CL, PC, Cer, SM, HexCer, Hex2Cer, and SulfoHexCer; and 50 V for LPI, and PI. For quantification of each lipid, 16 lipid (odd numbered carbon chain) standards of different lipid classes were added to each lipid extract sample as internal standards (IS). Amount of individual lipid was calculated as the corrected peak area which was the ratio of a specie's peak area to that of the IS (1 pmol per each injection) of the same lipid class. Statistical analysis of data was accomplished with Student's t-test, using SPSS software (version 24.0, IBM Corp., Armonk, NY, USA), and principal component analysis (PCA), using Minitab 17 statistical software (http://www.minitab.com).

2.7. Method validation

The limit of detection (LOD) and the limit of quantitation (LOQ) of the nUHPLC-ESI-MS/MS method were determined using plasma sample spiked with a set of lipid standards by varying injection amounts (0.025–3.0 pmol) based on the S/N = 3 and 10, respectively. Each measurement was made in triplicate. Calibration curves were established with the peak area vs. injection amount of individual lipid standard and LOD was based on the standard deviation of y-intercept.

3. Results

3.1. Size sorting of lipoproteins and lipid identification

Size separation of plasma lipoproteins by preparative scale AF4 channel is shown with the fractograms of the control, MCI, and AD patient plasma samples (50 μL each) in Fig. 1 obtained at 0.4 mL/min of outflow rate and 3.6 mL/min of crossflow rate. It appears that LDL and VLDL peak intensities of cognitively impaired groups (MCI and AD groups) are larger than those of age-matched healthy controls, supporting that the LDL and VLDL levels are elevated in the patient groups. While HDL and LDL were separated at the baseline under the applied run condition, LDL and VLDL were not completely resolved. Therefore, collections were made using HDL and a combined LDL/VLDL fraction. Lipids extracted from each lipoprotein fraction were analyzed by nUHPLC-ESI-MS/MS, at a run condition equivalent to the separation of lipid standards, as shown in Fig. S1 of Supplementary material. Ion chromatograms of lipid standards in Fig. S1 demonstrates the ultrahigh performance of lipid separation employed in this study which was enhanced by utilizing a homemade nUHPLC column packed with 1.7 μm reversed phase resin: 18.0 ± 9.6 s for the average peak width (based on 4σ) and 0.9 ± 0.5% for average RSD in retention time of all lipid standards, and 184,500 for the calculated plate number of $(14:0)_4$-CL. Identification of lipid molecular structure was based on data-dependent collision induced dissociation experiment of nUHPLC-ESI-MS/MS at the same run condition used in Fig. S1 and the base peak chromatograms of each lipoprotein fraction is shown in Fig. S2. LOD values (S/N = 3) were in the range of 0.059 (LPC)–0.507 pmol (LPG) and LOQ values (S/N = 10) were 0.197–1.689 pmol, respectively, based on the calibration curves in Fig. S3 and the calculated data are in Table S2. Non-targeted lipid identification was achieved with a pooled plasma sample from 13 controls, resulting in a listing of 363 lipids in Table S3.

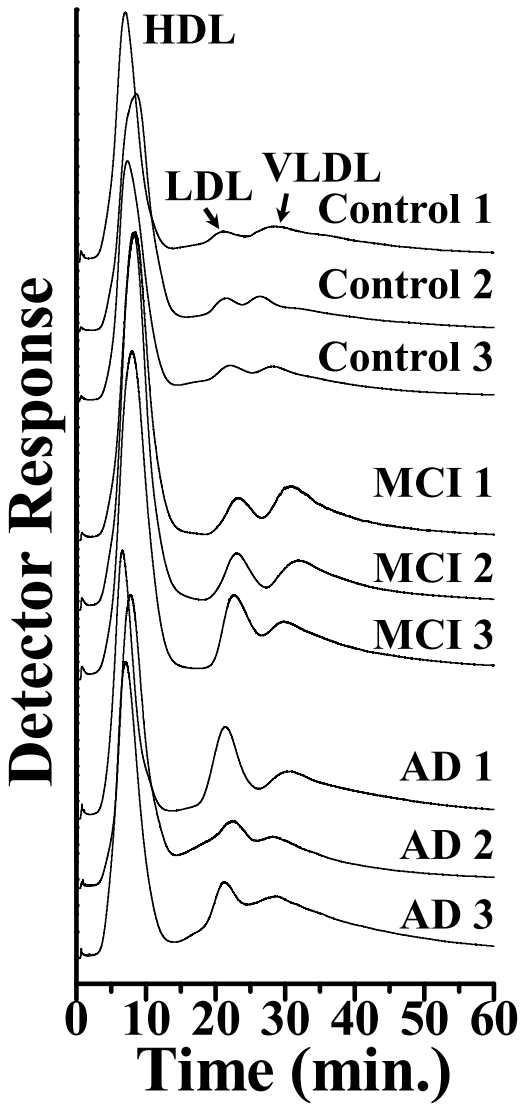

Fig. 1. Fractograms of individual plasma samples (controls and patients with MCI and AD) showing the size separation of HDL, LDL, and VLDL obtained by semi-prep asymmetrical flow field-flow fractionation at $\dot{V}_{in}/\dot{V}_{out}$ = 4.0/0.4 in. mL/min (50 μL injection for each plasma sample). Plasma lipoproteins were stained with Sudan Black B prior to separation.

3.2. Lipid alterations in MCI and AD

Quantification results of lipids for both HDL and LDL/VLDL fractions of 13 controls, 23 MCI, and 14 AD patient samples are listed in Table S3, with the corrected peak area (the ratio of peak area of individual lipid molecule to that of each internal standard (1 pmol) specific to lipid class), fold changes among the three groups, and relative abundance of each species within corresponding lipid class. In Fig. 2, the corrected peak areas of 8 different lipid classes, which showed more than 2-fold changes in either MCI or AD groups in HDL and LDL/VLDL, were compared using stacked bar graph. The remaining 6 lipid species were shown in Fig. S4. Lipids marked with acyl chain structures are high abundance species in each class, which is defined by a relative abundance higher than 100%/(number of lipids within the class). The "low" represents the summed amount of the low abundance species. Changes in the total level of each lipid class for MCI and AD patients are not noticeable in the HDL fraction except for the large decreases in DG and PG; however TG, PA, PI, PE, PEp, PG, Cer, and HexCer were significantly increased >2-fold in LDL/VLDL. Fig. 2 clearly shows that the level

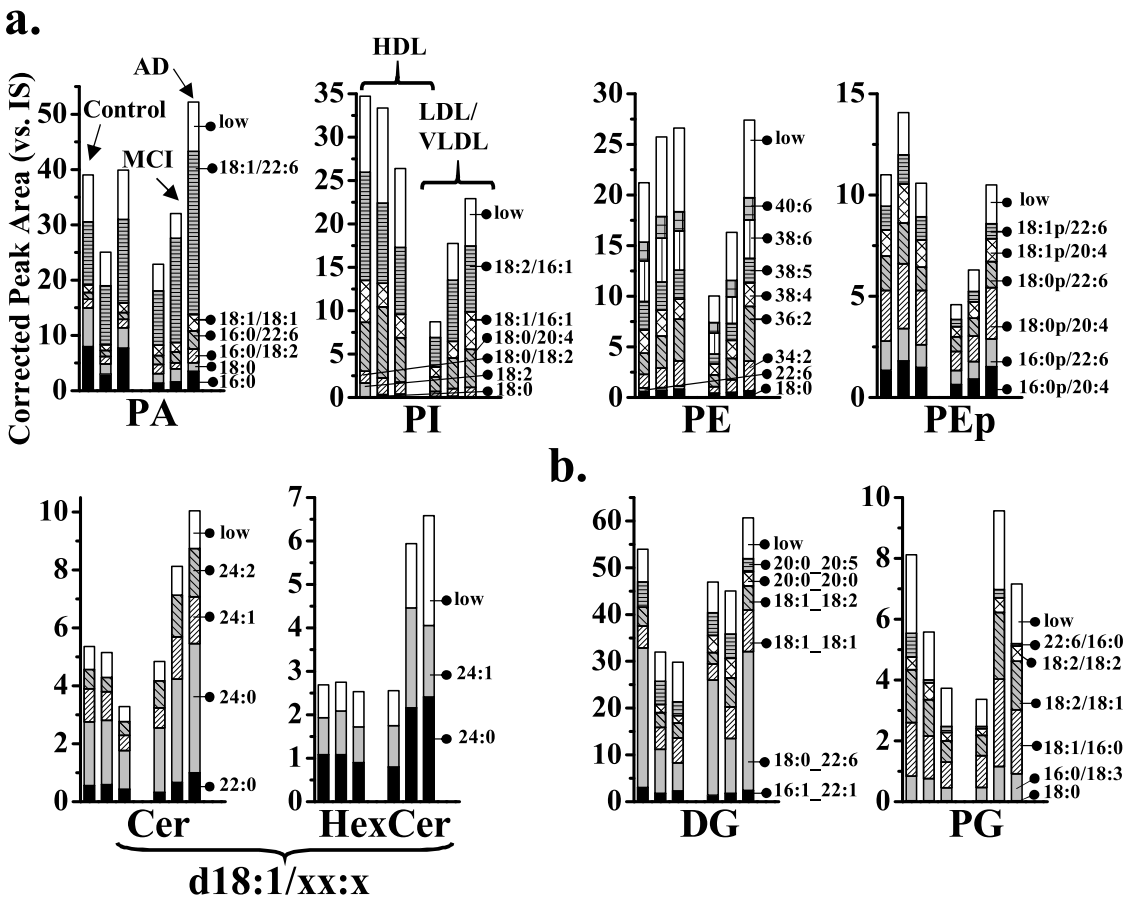

Fig. 2. Stacked bar graphs of individual lipid molecules in 8 lipid classes (based on the summation of corrected peak area) in HDL and LDL/VLDL fractions of control, MCI, and AD groups. Species with acyl chain structures are high abundance and the "low" represents the summed amount of low abundance species.

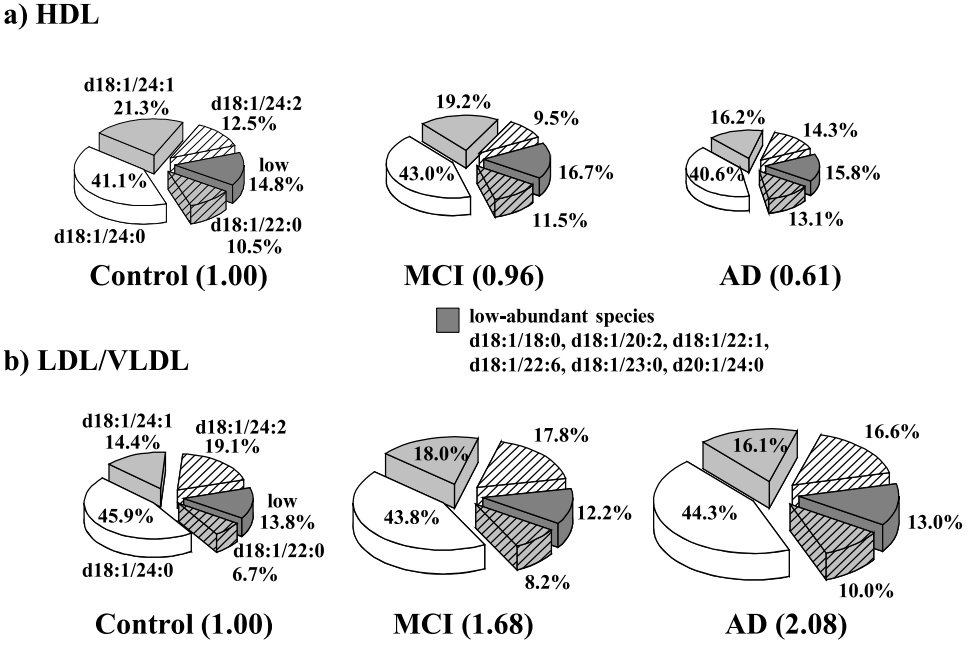

Fig. 3. Pie charts representing the compositional change in high abundant Cer species among control, MCI, and AD groups along with the relative abundance value by taking the control as the reference point of ï.00. The pie chart marked with "low" are for the summed amount of the six low abundant species as listed inside the figure.

change of lipids relies on the type of lipoproteins. Among the lipid classes showing a significant difference, alterations in the level of individual Cer species can be closely examined by plotting the pie charts in Fig. 3 in which the total amounts of Cer in MCI and AD are expressed with numbers relative to that of control (set as 1.00) as well as with the size variation of pie charts. Apparently, the total

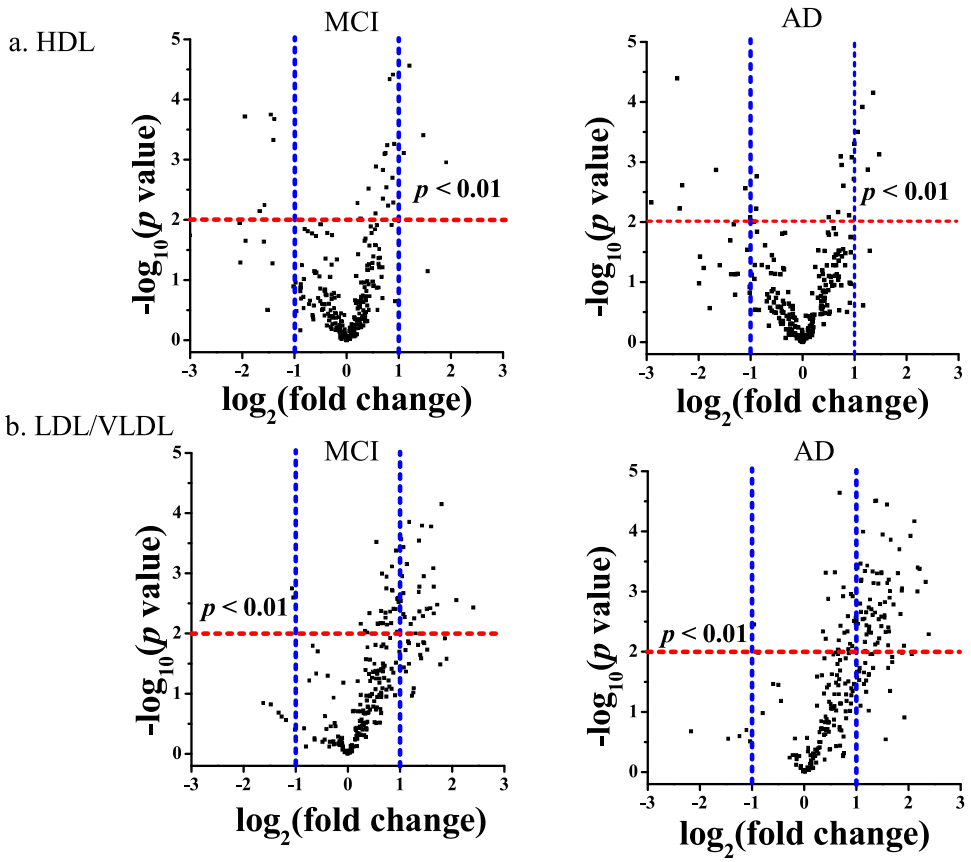

Fig. 4. Volcano plots of 363 lipid species representing $-\log_{10}$ (p value) vs. $\log_2$ (fold change) in MCI and AD groups in comparison to the control group.

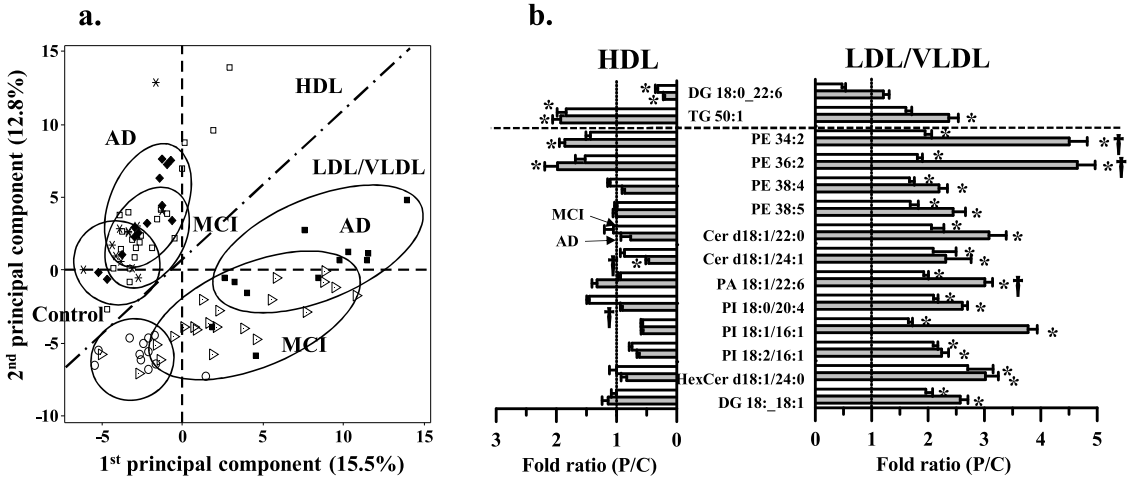

Fig. 5. a) PCA plots representing the differences in lipid profiles showing significant differences (>2-folds and $p < 0.01$ vs. controls) in MCI and AD (vs. controls) for HDL and LDL/VLDL fractions. Each symbol represents individual patient and b) selected high abundant lipid species with significant change ($p < 0.01$) in MCI (the top two for HDL and the remaining for LDL/VLDL) which are selected from lipid lists showing changes >2-folds with $p < 0.01$ in AD as listed Table 1. Species marked with * show a significant change ($p < 0.01$) from control and those with † represent for in AD vs. MCI.

amount of Cer in AD (0.61) decreased nearly two-folds in the HDL, but it increased about two-folds in the LDL/VLDL (2.08). In addition, the level of MCI shows a progressive increase from that of control in LDL/VLDL. Cer species marked with the molecular chain structures in Fig. 3 are the high abundant species out of total 10 identified species and their relative compositions were rather consistent with the development of AD in both lipoprotein fractions. The Cer level was reported to increase in the brain and CSF of AD because of the Aβ-mediated activation of sphingomyelinases, which convert SM to Cer [3,19,47]. In addition, Cer levels were increased in the insulin-resistant muscle of Zucker rats, related to diabetes rats [48]. The two Cers (d18:1/22:0 and d18:1/24:1) and HexCer d18:1/24:0 were found to significantly increase in the LDL/VLDL of both MCI and AD, supporting that circulating Cers carried by LDL occur in the stage of MCI. A similar comparison is found with DG in Fig. S5 showing that the entire DG level in HDL was largely decreased by ~2-fold in AD but increased approximately 30% in LDL/VLDL. However, the relative abundance of DG 18:1_18:1 increased by ~2-

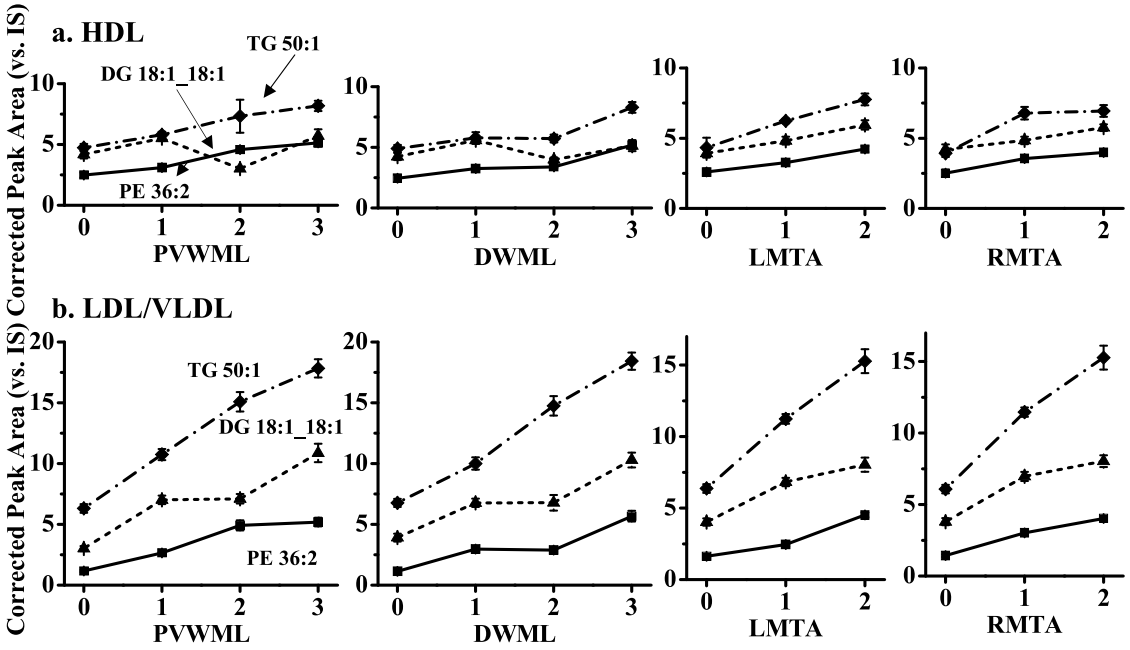

Fig. 6. Correlation of the three prominent lipid species (TG 50:1, DG 18:1_18:1, and PE 36:2) in a) HDL and b) LDL/VLDL with the rating of hyperintensity of deep white matter lesion (DWML), periventricular white matter lesion (PVWML), left medial temporal lobe atrophy (LMTA), and right medial temporal lobe atrophy (RMTA) measured by structural MRI.

fold in AD in both lipoprotein fractions with its level increased noticeably in LDL/VLDL, as 1.96-fold in MCI and 2.57-fold in AD vs. control. Such an increase is similar to the results found in both brain and plasma [18]. Because DG is known to correlate with insulin resistance as reported with its increase in muscle tissues of type 2 diabetes patients [32,49], increases of DG in AD patients support a close relationship between AD and diabetes [50]. Since the present study did not include patients with diabetes, DG increase from diabetic influence can be excluded.

The changes in the 363 individual lipid species can be illustrated with the Volcano plots, ($-\log_{10}$ (p value) vs. $\log_2$ (fold change)), in Fig. 4 showing that a considerable number of lipids were largely increased >2-fold and $p < 0.01$ (shown at the upper right domain of each plot) mostly in LDL/VLDL, for both MCI and AD. Therefore, lipids showing >2-fold and $p < 0.01$ were selected as a criteria for significant changes in the further investigations. The relative changes in individual lipids and in classes were visualized by plotting the heat map with significantly changed lipids (more than 2-fold changes either in MCI or AD vs. controls) in Fig. S6, representing clear increases of Cer, HexCer, Hex2Cer, DG, TG, PA, and PG species in the LDL/VLDL fraction.

Overall differences in plasma lipid profiles among patient groups are illustrated with the PCA plot in Fig. 5a for lipids with significant changes. Each data point in Fig. 5a represents the overall lipid profile of individual patient. While the differences among controls, MCI, and AD in the HDL fractions are not clear, data points in LDL/VLDL appear to cluster apart upon the progression to AD via MCI, supporting that alterations in lipid profiles in LDL/VLDL upon the progress of disease are more distinct than those in HDL. Among lipids in Table S3, high abundance species with significant changes either in HDL or LDL/VLDL are selected and listed in Table 1 with the fold ratio (MCI/control and AD/control), representing that most of them increased in LDL/VLDL of AD. Species marked with * represents significant difference ($p < 0.01$) from control. In Table 1, 14 lipids showing a progressive decrease or increase to AD (underlined fold ratio) were further selected as potential candidates that can be comprehensively investigated in the future for the possible early detection of MCI. The fold changes of the fourteen lipid species are plotted by bar graphs in Fig. 5b showing large increases only in LDL/VLDL, except for DG 18:0_22:6 (decrease in HDL) and TG 50:1 (increases in both fractions).This supports the strong dependence of the disease progress on lipid levels in LDL/VLDL fraction. Significant increases (approximately 2–4.5 times in AD) of the four high abundance PE levels in LDL/VLDL in Fig. 5b may be correlated with AD pathogenesis since a report showed that knock-out of PE synthesis resulted in decreased Aβ in mammalian cells by promoting α-secretase and deactivating γ-secretase [51].

3.3. Correlation of lipids with brain pathological results

To investigate the potential of the above selected lipids as candidate species reflecting brain pathologies, we examined the relationship between alterations of the14 lipid species in Fig. 5b and brain atrophy, a hallmark of AD pathology regardless of the diagnosis, resulting in the strong correlation with the three lipids (TG 50:1, DG 18:1_18:1, and PE 36:2) in Fig. 6. It revealed that the lipid levels in HDL moderately increased with the degree of lesion (PVWML and DWML) and atrophy (left medial temporal lobe atrophy (LMTA) and right medial temporal lobe atrophy (RMTA)) in Fig. 6a; however, they largely increased by 2–4-fold in LDL/VLDL in Fig. 6b, supporting that these three lipids are closely associated with the brain damage. Furthermore, the receiver operating characteristic (ROC) curve was plotted for the lipid levels in the LDL/VLDL of the MCI group, in contrast with controls. When lipid changes in MCI group were incorporated in combination with the scores of mini-mental state examination (MMSE), neuropsychiatric interview to measure cognitive impairment, the area under curve (AUC) values of the three lipid species increased to 0.833 for TG 50:1, 0.847 for DG 18:1_18:1, and 0.917 for PE 36:2 from 0.800 for MMSE alone in Fig. 7. This conforms to the philosophy of recently proposed diagnostic criteria that suggest a way of increasing the reliability of clinical diagnosis of MCI by engaging supporting evidence of known biomarkers, MMSE. Though the remaining 11 lipid species did not show a strong correlation with brain atrophy, their AUC values in combination with MMSE were significantly larger than 0.800 as follows: PE 34:2 (0.861), PE 38:4 (0.873), PE 38:5 (0.892), PA

Table 1
Fold ratio (vs. control) of high abundance lipid species showing a significant change (>2-folds, $p < 0.01$) either in high-density lipoprotein (HDL) or low-density lipoprotein (LDL)/very low-density lipoprotein (VLDL) fractions from the patient groups of mild cognitive impairment (MCI) and Alzheimer's disease (AD) (vs. control). Percentage value is the relative abundance in each lipid class. Fold ratio marked with bold in AD represents >2-folds, with * for $p < 0.01$, and with underline for characteristic lipid species of MCI under progressive increase of decrease to AD.

Class	Chain	*m/z*	HDL			LDL/VLDL		
			MCI / Control	AD/Control	(%)	MCI/Control	AD/Control	(%)
LPC	16:0	496.5	0.71 ± 0.03	1.00 ± 0.05	48.84	1.34 ± 0.05	**2.13 ± 0.10***	36.59
PE	**34:2**	716.5	1.43 ± 0.07	1.86 ± 0.09*	6.90	1.95 ± 0.12*	**4.50 ± 0.32***	6.93
	36:2	744.5	1.52 ± 0.16	1.98 ± 0.21*	10.70	1.81 ± 0.09*	**4.65 ± 0.31***	12.31
	38:4	768.5	1.10 ± 0.04	0.87 ± 0.04	11.84	1.67 ± 0.09*	**2.19 ± 0.15***	11.36
	38:5	766.5	0.99 ± 0.05	1.01 ± 0.05	14.48	1.68 ± 0.14*	**2.44 ± 0.22***	10.43
	40:6	792.5	1.15 ± 0.06	1.02 ± 0.05	9.65	1.57 ± 0.13	**2.10 ± 0.18***	11.01
PEp	16:0p/20:4	724.5	1.34 ± 0.08	1.11 ± 0.06	12.27	1.44 ± 0.09	**2.38 ± 0.16***	14.00
	18:0p/20:4	752.5	1.28 ± 0.12	1.07 ± 0.08	22.78	1.34 ± 0.08	**2.69 ± 0.17***	20.63
LPA	16:0	409.5	0.38 ± 0.01*	0.97 ± 0.04	43.87	1.18 ± 0.04	**2.57 ± 0.13***	42.84
LPA	18:0	437.5	0.26 ± 0.02*	**0.52 ± 0.04***	38.36	1.38 ± 0.09	0.90 ± 0.06	52.81
PA	**18:1/22:6**	745.5	0.93 ± 0.04	1.32 ± 0.08	54.68	1.92 ± 0.08*	**3.01 ± 0.14***	49.98
PG	16:0/18:3	743.5	0.90 ± 0.04	0.53 ± 0.03	10.05	2.59 ± 0.19*	**2.04 ± 0.14***	12.98
	18:1/16:0	747.5	0.80 ± 0.03	0.48 ± 0.02	21.74	2.74 ± 0.12*	**2.00 ± 0.09***	31.59
	18:2/18:1	771.5	0.69 ± 0.03	0.40 ± 0.02	21.56	3.28 ± 0.19*	**2.40 ± 0.15***	20.02
LPI	18:2	595.5	0.09 ± 0.01*	**0.19 ± 0.01***	85.4	0.72 ± 0.05	0.36 ± 0.03	21.83
PI	**18:0/20:4**	885.5	1.45 ± 0.04	0.90 ± 0.03	17.17	2.10 ± 0.08*	**2.61 ± 0.09***	19.84
	18:1/16:1	833.5	0.56 ± 0.03	0.56 ± 0.03	14.74	1.65 ± 0.08*	**3.77 ± 0.16***	13.55
	18:2/16:1	831.5	0.74 ± 0.05	0.62 ± 0.04	37.97	2.09 ± 0.08*	**2.24 ± 0.12***	39.68
Cer	**d18:1/22:0**	622.5	1.05 ± 0.15	0.77 ± 0.16	10.48	2.06 ± 0.22*	**3.08 ± 0.31***	6.71
	d18:1/24:0	650.5	1.01 ± 0.14	0.61 ± 0.08	40.99	1.60 ± 0.11	**2.01 ± 0.12***	45.88
	d18:1/24:1	648.5	0.87 ± 0.07	**0.47 ± 0.05***	21.28	2.09 ± 0.41*	**2.31 ± 0.45***	14.45
HexCer	**d18:1/24:0**	812.5	1.00 ± 0.12	0.83 ± 0.10	40.36	2.70 ± 0.45*	**3.02 ± 0.23***	31.33
Hex2Cer	d18:1/24:1	972.5	0.74 ± 0.07	0.87 ± 0.07	48.04	1.59 ± 0.13	**2.29 ± 0.21***	19.36
DG	**18:0_22:6**	686.5	0.31 ± 0.04*	**0.20 ± 0.02***	55.20	0.47 ± 0.06*	1.21 ± 0.11	52.48
	18:1_18:1	638.5	1.00 ± 0.09	1.14 ± 0.10	8.67	1.96 ± 0.12*	**2.57 ± 0.14***	7.33
	18:1_18:2	636.5	0.77 ± 0.05	0.78 ± 0.05	7.51	2.57 ± 0.13*	**2.14 ± 0.09***	5.16
TG	**50:1**	850.8	1.84 ± 0.15*	1.93 ± 0.14*	4.37	1.61 ± 0.10	**2.37 ± 0.17***	4.65
	50:2	848.8	1.28 ± 0.07	**2.39 ± 0.14***	2.99	1.42 ± 0.09	1.80 ± 0.13	3.81

Abbreviations: Cer, ceramide; LPA, lysophosphatidic acid; LPC, lysophosphatidylcholine; LPI, lysophosphatidylinositol; HexCer, monohexosylceramide; Hex2Cer, dihexosylceramide; PA, phosphatidic acid; PC, phosphatidylcholine; PE, phosphatidylethanolamine; Pep, PE plasmalogen; PG, phosphatidylglycerol; PI, phosphatidylinositol; DG, diacylglycerol; TG, triacylglycerol.

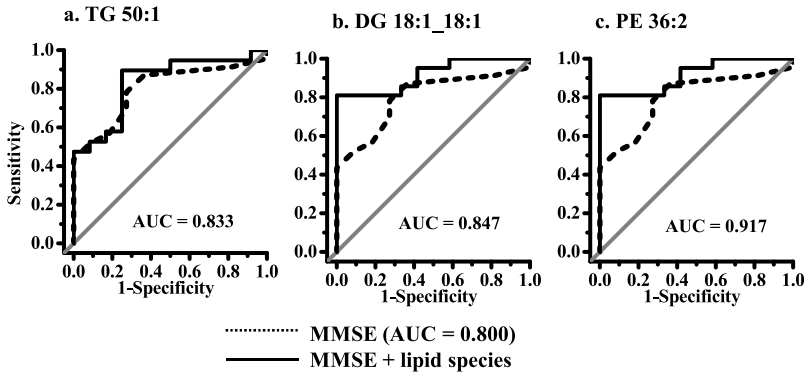

Fig. 7. ROC curves of the four candidate markers, a) TG 50:1, b) DG 18:1_18:1, c) PA 18:1/22:6, and d) PE 36:2 in MCI in combination with MMSE scores (solid line) superimposed with those of MMSE scores alone (dotted line).

18:1/22:6 (0.880), Cer d18:1/22:0 (0.918), Cer d18:1/24:1 (0.938), PI 18:0/20:4 (0.909), PI 18:1/16:1 (0.862), PI 18:2/16:1 (0.887), HexCer d18:1/24:0 (0.905), and DG 18:0_22:6 (0.907). These results strongly suggest the potential of these molecules are promising peripheral candidates as a method to increase the reliability of clinical diagnosis of MCI provided with the validation.

4. Conclusions

The present study shows that lipid analysis of entire blood samples without lipoprotein separation may not reveal the perturbed changes in the development of AD, as is also reported by the evidence of cholesterols in HDL-C and LDL-C associating with Aβ levels [52]. Although the mechanisms of alterations in individual lipid levels related to AD development are not yet known, the observed changes in lipid levels reveal that not all lipids in the same class show a same trend of changes and a systematic investigation of lipid expression in different lipoproteins is essential to enrich the knowledge of the progression of MCI and AD. It is shown that the 28 plasma lipid species in Table 1 were significantly altered in AD and the three lipid species (TG 50:1, DG 18:1_18:1, and PE 36:2) having a strong correlation with brain degenerative changes of MCI revealed and improved selectivity in differentiating MCI when incorporated with the common test scores of cognitive impairments. This also means that blood-based lipids, which are readily accessible, rather than neuroimaging or CSF biomarkers, could be used to facilitate the validity of mass screening for dementia risk with combined use of the simple and brief tool, MMSE. Further studies are required

to validate the candidate lipid species found in this study toward the detection of the very early stages of MCI with the required specificity.

Disclosure statement

The authors report no actual or potential conflict of interest.

Acknowledgements

This study was supported by a grant (NRF-2015R1A2A1A01004677) through the National Research Foundation (NRF) of Korea, funded by the Ministry of Science, ICT & Future Planning.

Appendix A. Supplementary data

Supplementary material related to this article can be found, in the online version, at doi:https://doi.org/10.1016/j.chroma.2018.07.018.

References

[1] J.J. Palop, L. Mucke, Amyloid-B-induced neuronal dysfunction in Alzheimer's disease: from synapses toward neural networks, Nat. Neurosci. 13 (2010) 812–818.
[2] R.A. Huynh, C. Mohan, Alzheimer's disease: biomarkers in the genome, blood, and cerebrospinal fluid, Front. Neurol. 8 (2017).
[3] M.O.W. Grimm, J. Mett, H.S. Grimm, T. Hartmann, APP function and lipids: a bidirectional link, Front. Mol. Neurosci. 10 (2017).
[4] B.A. Yankner, New clues to Alzheimer's disease: unraveling the roles of amyloid and tau, Nat. Med. 2 (1996) 850–852.
[5] I. Grundke-Iqbal, K. Iqbal, M. Quinlan, Y.C. Tung, M.S. Zaidi, H.M. Wisniewski, Microtubule-associated protein tau. A component of Alzheimer paired helical filaments, J. Biol. Chem. 261 (1986) 6084–6089.
[6] R.C. Petersen, R. Doody, a Kurz, R.C. Mohs, J.C. Morris, P.V. Rabins, K. Ritchie, M. Rossor, L. Thal, B. Winblad, Current concepts in mild cognitive impairment, Arch. Neurol. 58 (2001) 1985–1992.
[7] S. Galluzzi, C. Geroldi, G. Amicucci, L. Bocchio-Chiavetto, M. Bonetti, C. Bonvicini, M. Cotelli, R. Ghidoni, B. Paghera, O. Zanetti, G.B. Frisoni, S. Archetti, L. Benussi, G. Binetti, E. Canu, F. Caobelli, E. Cavedo, E. Chitò, D. Costardi, M. Gennarelli, R. Giubbini, U.P. Guerra, G. Kuffenschin, G. Lussignoli, D. Moretti, A. Orlandini, M. Parapini, D. Paternicò, C. Porteri, M. Romano, S. Rosini, C. Scarpazza, I. Villa, R. Zanardini, Supporting evidence for using biomarkers in the diagnosis of MCI due to AD, J. Neurol. 260 (2013) 640–650.
[8] M. Björkqvist, M. Ohlsson, L. Minthon, O. Hansson, Evaluation of a previously suggested plasma biomarker panel to identify Alzheimer's disease, PLoS One 7 (2012).
[9] S. Ray, M. Britschgi, C. Herbert, Y. Takeda-Uchimura, A. Boxer, K. Blennow, L.F. Friedman, D.R. Galasko, M. Jutel, A. Karydas, J.A. Kaye, J. Leszek, B.L. Miller, L. Minthon, J.F. Quinn, G.D. Rabinovici, W.H. Robinson, M.N. Sabbagh, Y.T. So, D.L. Sparks, M. Tabaton, J. Tinklenberg, J.A. Yesavage, R. Tibshirani, T. Wyss-Coray, Classification and prediction of clinical Alzheimer's diagnosis based on plasma signaling proteins, Nat. Med. 13 (2007) 1359–1362.
[10] E. Kapaki, G.P. Paraskevas, I. Zalonis, C. Zournas, CSF tau protein and β-amyloid (1-42) in Alzheimer's disease diagnosis: discrimination from normal ageing and other dementias in the Greek population, Eur. J. Neurol. 10 (2003) 119–128.
[11] C. Humpel, Identifying and validating biomarkers for Alzheimer's disease, Trends Biotechnol. 29 (2011) 26–32.
[12] C.M. Karch, A.T. Jeng, A.M. Goate, Extracellular tau levels are influenced by variability in tau that is associated with tauopathies, J. Biol. Chem. 287 (2012) 42751–42762.
[13] L.M. Shaw, H. Vanderstichele, M. Knapik-Czajka, C.M. Clark, P.S. Aisen, R.C. Petersen, K. Blennow, H. Soares, A. Simon, P. Lewczuk, R. Dean, E. Siemers, W. Potter, V.M.Y. Lee, J.Q. Trojanowski, Cerebrospinal fluid biomarker signature in Alzheimer's disease neuroimaging initiative subjects, Ann. Neurol. 65 (2009) 403–413.
[14] A. Hye, J. Riddoch-Contreras, A.L. Baird, N.J. Ashton, C. Bazenet, R. Leung, E. Westman, A. Simmons, R. Dobson, M. Sattlecker, M. Lupton, K. Lunnon, A. Keohane, M. Ward, I. Pike, H.D. Zucht, D. Pepin, W. Zheng, A. Tunnicliffe, J. Richardson, S. Gauthier, H. Soininen, I. Kłoszewska, P. Mecocci, M. Tsolaki, B. Vellas, S. Lovestone, Plasma proteins predict conversion to dementia from prodromal disease, Alzheimer's Dement. 10 (2014) 799–807.
[15] A. Hye, S. Lynham, M. Thambisetty, M. Causevic, J. Campbell, H.L. Byers, C. Hooper, F. Rijsdijk, S.J. Tabrizi, S. Banner, C.E. Shaw, C. Foy, M. Poppe, N. Archer, G. Hamilton, J. Powell, R.G. Brown, P. Sham, M. Ward, S. Lovestone, Proteome-based plasma biomarkers for Alzheimer's disease, Brain 129 (2006) 3042–3050.
[16] S.J. Lee, U. Liyanage, P.E. Bickel, W. Xia, P.T. Lansbury, K.S. Kosik, A detergent-insoluble membrane compartment contains Aβ in vivo, Nat. Med. 4 (1998) 730–734.
[17] D.R. Riddell, G. Christie, I. Hussain, C. Dingwall, Compartmentalization of β-secretase (Asp2) into low-buoyant density, noncaveolar lipid rafts, Curr. Biol. 11 (2001) 1288–1293.
[18] X. Han, D.M. Holtzman, D.W. McKeel, Plasmalogen deficiency in early Alzheimer's disease subjects and in animal models: molecular characterization using electrospray ionization mass spectrometry, J. Neurochem. 77 (2001) 1168–1180.
[19] X. Han, D. Holtzman, D.W. McKeel, J. Kelley, J.C. Morris, Substantial sulfatide deficiency and ceramide elevation in very early Alzheimer's disease: potential role in disease pathogenesis, J. Neurochem. 82 (2002) 809–818.
[20] P.L. Wood, S. Medicherla, N. Sheikh, B. Terry, A. Phillipps, J.A. Kaye, J.F. Quinn, R.L. Woltjer, Targeted lipidomics of fontal cortex and plasma diacylglycerols (DAG) in mild cognitive impairment and Alzheimer's disease: validation of DAG accumulation early in the pathophysiology of Alzheimer's disease, J. Alzheimer's Dis. 48 (2015) 537–546.
[21] P. Proitsi, M. Kim, L. Whiley, A. Simmons, M. Sattlecker, L. Velayudhan, M.K. Lupton, H. Soininen, I. Kloszewska, P. Mecocci, M. Tsolaki, B. Vellas, S. Lovestone, J.F. Powell, R.J.B. Dobson, C. Legido-Quigley, Association of blood lipids with Alzheimer's disease: a comprehensive lipidomics analysis, Alzheimer's Dement. 13 (2016) 1–12.
[22] Y.M. Kuo, M.R. Emmerling, C.L. Bisgaier, A.D. Essenburg, H.C. Lampert, D. Drumm, A.E. Roher, Elevated low-density lipoprotein in Alzheimer's disease correlates with brain aβ 1-42 levels, Biochem. Biophys. Res. Commun. 252 (1998) 711–715.
[23] X. Han, R.W. Gross, Structural determination of picomole amounts of phospholipids via electrospray ionization tandem mass spectrometry, J. Am. Soc. Mass Spectrom. 6 (1995) 1202–1210.
[24] R. Schneiter, B. Brügger, R. Sandhoff, G. Zellnig, A. Leber, M. Lampl, K. Athenstaedt, C. Hrastnik, S. Eder, G. Daum, F. Paltauf, F.T. Wieland, S.D. Kohlwein, Electrospray ionization tandem mass spectrometry (ESI-MS/MS) analysis of the lipid molecular species composition of yeast subcellular membranes reveals acyl chain-based sorting/remodeling of distinct molecular species en route to the plasma membrane, J. Cell Biol. 146 (1999) 741–754.
[25] R. Taguchi, J. Hayakawa, Y. Takeuchi, M. Ishida, Two-dimensional analysis of phospholipids by capillary liquid chromatography/electrospray ionization mass spectrometry, J. Mass Spectrom. 35 (2000) 953–966.
[26] G. Isaac, D. Bylund, J.-E. Månsson, K.E. Markides, J. Bergquist, Analysis of phosphatidylcholine and sphingomyelin molecular species from brain extracts using capillary liquid chromatography electrospray ionization mass spectrometry, J. Neurosci. Methods 128 (2003) 111–119.
[27] M. Li, L. Yang, Y. Bai, H. Liu, Analytical methods in lipidomics and their applications, Anal. Chem. 86 (2014) 161–175.
[28] T. Cajka, O. Fiehn, Comprehensive analysis of lipids in biological systems by liquid chromatography–mass spectrometry, TrAC—Trends Anal. Chem. 61 (2014) 192–206.
[29] U. Sommer, H. Herscovitz, F.K. Welty, C.E. Costello, LC–MS-based method for the qualitative and quantitative analysis of complex lipid mixtures, J. Lipid Res. 47 (2006) 804–814.
[30] M. Lísa, M. Holčapek, High-throughput and comprehensive lipidomic analysis using ultrahigh-performance supercritical fluid chromatography-mass spectrometry, Anal. Chem. 87 (2015) 7187–7195.
[31] H. Nie, R. Liu, Y. Yang, Y. Bai, Y. Guan, D. Qian, T. Wang, H. Liu, Lipid profiling of rat peritoneal surface layers by online normal- and reversed-phase 2D LC QToF-MS, J. Lipid Res. 51 (2010) 2833–2844.
[32] S.K. Byeon, J.C. Lee, B.C. Chung, H.S. Seo, M.H. Moon, High-throughput and rapid quantification of lipids by nanoflow UPLC-ESI-MS/MS: application to the hepatic lipids of rabbits with nonalcoholic fatty liver disease, Anal. Bioanal. Chem. 408 (2016) 4975–4985.
[33] S.K. Byeon, J.Y. Kim, J.Y. Lee, B.C. Chung, H.S. Seo, M.H. Moon, Top-down and bottom-up lipidomic analysis of rabbit lipoproteins under different metabolic conditions using flow field-flow fractionation, nanoflow liquid chromatography and mass spectrometry, J. Chromatogr. A 1405 (2015) 140–148.
[34] J.C. Lee, I.Y. Kim, Y. Son, S.K. Byeon, D.H. Yoon, J.S. Son, H.S. Song, W. Song, J.K. Seong, M.H. Moon, Evaluation of treadmill exercise effect on muscular lipid profiles of diabetic fatty rats by nanoflow liquid chromatography-tandem mass spectrometry, Sci. Rep. 6 (2016).
[35] J.Y. Lee, S.K. Byeon, M.H. Moon, Profiling of oxidized phospholipids in lipoproteins from patients with coronary artery disease by hollow fiber flow field-flow fractionation and nanoflow liquid chromatography-tandem mass spectrometry, Anal. Chem. 87 (2015) 1266–1273.
[36] P.R. Wenham, W.H. Price, G. Blundell, Apolipoprotein E genotyping by one-stage PCR, Lancet 337 (1991) 1158–1159.
[37] American Psychiatric Association, Diagnostic and Statistical Manual of Mental Disorders, 2000.
[38] D.Y. Lee, K.U. Lee, J.H. Lee, K.W. Kim, J.H. Jhoo, S.Y. Kim, J.C. Yoon, S.I. Woo, J. Ha, J.I. Woo, A normative study of the CERAD neuropsychological assessment battery in the Korean elderly, J. Int. Neuropsychol. Soc. 10 (2004) 72–81.
[39] J.H. Lee, K.U. Lee, D.Y. Lee, K.W. Kim, J.H. Jhoo, J.H. Kim, K.H. Lee, S.Y. Kim, S.H. Han, J.I. Woo, Development of the Korean version of the consortium to establish a registry for Alzheimer's disease assessment packet (CERAD-K): clinical and neuropsychological assessment batteries, J. Gerontol. Ser. B: Psychol. Sci. Soc. Sci. 57 (2002) P47–P53.

[40] J.C. Moms, A. Heyman, R.C. Mohs, J.P. Hughes, G. van Belle, G. Fillenbaum, E.D. Mellits, C. Clark, The consortium to establish a registry for Alzheimer's disease (CERAD). Part I. Clinical and neuropsychological assesment of Alzheimer's disease, Neurology 39 (1989) 1159.
[41] G. McKhann, D. Drachman, M. Folstein, R. Katzman, D. Price, E.M. Stadlan, Clinical diagnosis of Alzheimer's disease: report of the NINCDS-ADRDA Work Group* under the auspices of Department of Health and Human Services Task Force on Alzheimer's Disease, Neurology 34 (1984) 939.
[42] R.C. Petersen, G.E. Smith, S.C. Waring, R.J. Ivnik, E. Kokmen, E.G. Tangelos, Aging, memory, and mild cognitive impairment, Int. Psychogeriatr. 9 (1997) 65–69.
[43] P. Scheltens, D. Leys, F. Barkhof, D. Huglo, H.C. Weinstein, P. Vermersch, M. Kuiper, M. Steinling, E.C. Wolters, J. Valk, Atrophy of medial temporal lobes on MRI in "probable" Alzheimer's disease and normal ageing: diagnostic value and neuropsychological correlates, J. Neurol. Neurosurg. Psychiatry 55 (1992) 967–972.
[44] F. Fazekas, J.B. Chawluk, A. Alavi, MR signal abnormalities at 1.5 T in Alzheimer's dementia and normal aging, Am. J. Neuroradiol. 8 (1987) 421–426.
[45] S.K. Byeon, J.Y. Lee, M.H. Moon, Optimized extraction of phospholipids and lysophospholipids for nanoflow liquid chromatography-electrospray ionization-tandem mass spectrometry, Analyst 137 (2012) 451–458.
[46] S. Lim, S.K. Byeon, J.Y. Lee, M.H. Moon, Computational approach to structural identification of phospholipids using raw mass spectra from nanoflow liquid chromatography-electrospray ionization-tandem mass spectrometry, J. Mass Spectrom. 47 (2012) 1004–1014.
[47] A. Jana, K. Pahan, Fibrillar amyloid-β peptides kill human primary neurons via NADPH oxidase-mediated activation of neutral sphingomyelinase: implications for Alzheimer's disease, J. Biol. Chem. 279 (2004) 51451–51459.
[48] W.L. Holland, J.T. Brozinick, L.P. Wang, E.D. Hawkins, K.M. Sargent, Y. Liu, K. Narra, K.L. Hoehn, T.A. Knotts, A. Siesky, D.H. Nelson, S.K. Karathanasis, G.K.K. Fontenot, M.J. Birnbaum, S.A. Summers, Inhibition of ceramide synthesis ameliorates glucocorticoid-, saturated-fat-, and obesity-induced insulin resistance, Cell Metab. 5 (2007) 167–179.
[49] S. Timmers, P. Schrauwen, J. de Vogel, Muscular diacylglycerol metabolism and insulin resistance, Physiol. Behav. 94 (2008) 242–251.
[50] A. Ott, R.P. Stolk, F. van Harskamp, H.A. Pols, A. Hofman, M.M. Breteler, Diabetes mellitus and the risk of dementia: the Rotterdam Study, Neurology 53 (1999) 1937–1942.
[51] I. Nesic, F.X. Guix, K. Vennekens, V. Michaki, P.P. Van Veldhoven, F. Feiguin, B. De Strooper, C.G. Dotti, T. Wahle, Alterations in phosphatidylethanolamine levels affect the generation of Aβ, Aging Cell 11 (2012) 63–72.
[52] B. Reed, S. Villeneuve, W. Mack, C. DeCarli, H.C. Chui, W. Jagust, Associations between serum cholesterol levels and cerebral amyloidosis, JAMA Neurol. 71 (2014) 195–200.